Distinct contributions of metabolic dysfunction and genetic risk factors in the pathogenesis of non-alcoholic fatty liver disease

Panu K. Luukkonen, Sami Qadri, Noora Ahlholm, Kimmo Porthan, Ville Männistö, Henna Sammalkorpi, Anne K. Penttilä, Antti Hakkarainen, Tiina E. Lehtimäki, Melania Gaggini, Amalia Gastaldelli, Mika Ala-Korpela, Marju Orho-Melander, Johanna Arola, Anne Juuti,Jussi Pihlajamäki, Leanne Hodson, Hannele Yki-Järvinen

Table of contents

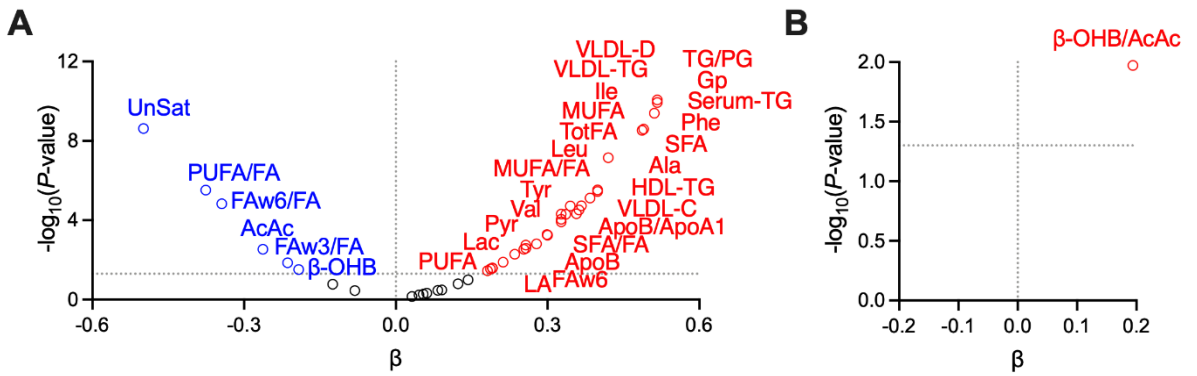

Fig. S1. Associations of 'MetComp' and 'GenComp' with metabolomics after excluding individuals with diabetes. (**A**) A volcano plot showing linear regression between HOMA-IR and NMR metabolomics variables that were included in PC1, 5, 6, 7 and 11, adjusted for age, sex, BMI, lipid-lowering medication and GRS after excluding individuals with diabetes from the *Discovery cohort*. (**B**) A volcano plot showing linear regression between GRS and NMR metabolomics variables that were included in PC9, adjusted for age, sex, BMI, lipid-lowering medication and HOMA-IR after excluding individuals with diabetes from the *Discovery cohort*. β-OHB/AcAc, β-hydroxybutyrate/acetoacetate ratio. Red denotes a positive and blue a negative correlation. Multiple testing was corrected by the Benjamini-Hochberg method.

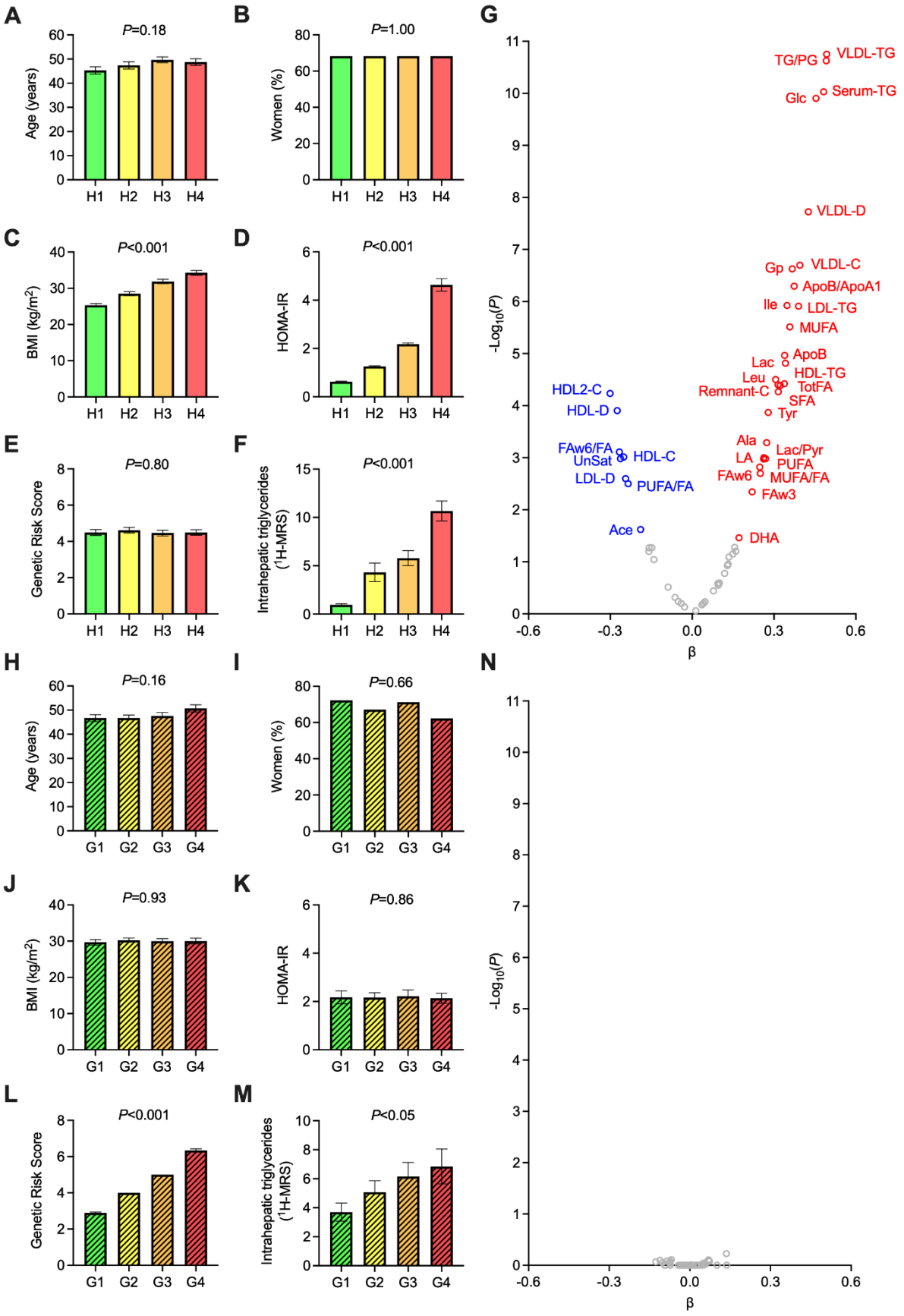
A
P=0.18
Age (years)
H1 H2 H3 H4
B
P=1.00
Women (%)
C
P<0.001
BMI (kg/m²)
D
P<0.001
HOMA-IR
E
P=0.80
Genetic Risk Score
F
P<0.001
Intrahepatic triglycerides (¹H-MRS)
G
-Log10(P)
β
TG/PG
VLDL-TG
Glc
Serum-TG
VLDL-D
Gp
VLDL-C
ApoB/ApoA1
Ile
LDL-TG
MUFA
Lac
ApoB
Leu
HDL-TG
Remnant-C
TotFA
SFA
HDL2-C
HDL-D
Tyr
Ala
Lac/Pyr
FAw6/FA
UnSat
HDL-C
LA
PUFA
LDL-D
PUFA/FA
FAw6
MUFA/FA
FAw3
Ace
DHA
H
P=0.16
Age (years)
G1 G2 G3 G4
I
P=0.66
Women (%)
J
P=0.93
BMI (kg/m²)
K
P=0.86
HOMA-IR
L
P<0.001
Genetic Risk Score
M
P<0.05
Intrahepatic triglycerides (¹H-MRS)
N
-Log10(P)
β

Fig. S2. 'MetComp' but not 'GenComp' associates with substrate surplus in the *Non-bariatric cohort.* (**A**) Age, (**B**) sex, (**C**) BMI, (**D**) HOMA-IR, (**E**) genetic risk score (GRS), (**F**) IHTGs in non-diabetic individuals divided into quartiles based on sex-specific HOMA-IR (*H1-H4*, n=63 in each group). (**G**) A volcano plot showing linear regression between HOMA-IR and NMR metabolomics variables, adjusted for age, sex, BMI, lipid-lowering medication and GRS in the *Non-bariatric cohort*. (**H**) Age, (**I**) sex, (**J**) BMI, (**K**) HOMA-IR, (**L**) GRS, (**M**) IHTGs in non-diabetic individuals divided into groups based on the GRS (*G1*, 2-3 risk alleles, n=54; *G2*, 4 risk alleles, n=79; *G3*, 5 risk alleles, n=66; *G4*, 6-7 risk alleles, n=53). (**N**) A volcano plot showing linear regression between GRS and NMR metabolomics variables, adjusted for age, sex, BMI, lipid-lowering medication and HOMA-IR in the *Non-bariatric cohort*. Red denotes a positive and blue a negative correlation. Multiple testing was corrected by the Benjamini-Hochberg method.

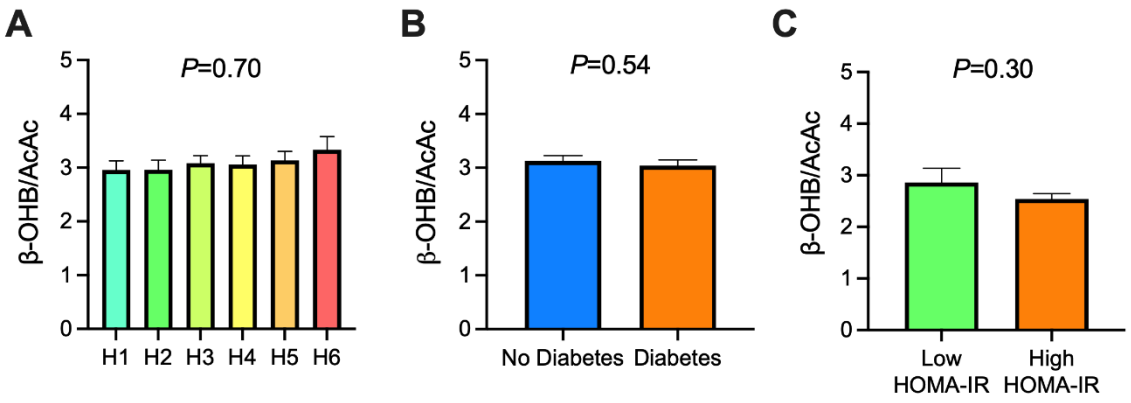

Fig. S3. No association between hepatic mitochondrial redox state and IR or diabetes in the present study. (**A**) β-hydroxybutyrate/acetoacetate ratios (β-OHB/AcAc) in groups based on sex-specific HOMA-IR (*H1-H6*) in the Discovery cohort. Significance was determined by the Kruskal-Wallis analysis of variance test. (**B**) β-OHB/AcAc in individuals with and without diabetes in the *Discovery cohort*. (**C**) β-OHB/AcAc in groups with HOMA-IR either below ('Low HOMA-IR') or above ('High HOMA-IR') the sex-specific median in the *DNL cohort*. Significances were determined by unpaired, two-tailed t-test.

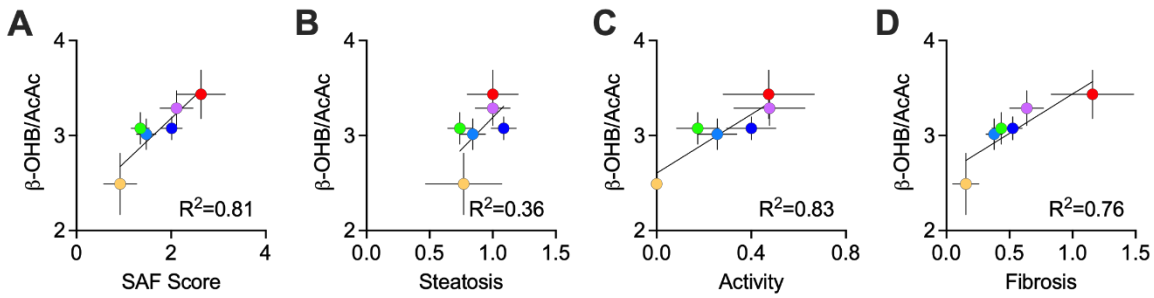

Fig. S4. Histological features of NAFLD are proportional to the hepatic mitochondrial redox state in groups with different number of risk alleles. Linear regressions between average β-hydroxybutyrate/acetoacetate ratio (β-OHB/AcAc) and average (**A**) SAF score, (**B**) steatosis, (**C**) activity and (**D**) fibrosis in groups based on the genetic risk score. Each dot denotes the mean and whiskers denote standard errors. Colors in denote the number of risk-increasing alleles: yellow, 1-2; green, 3; light blue, 4; dark blue, 5; pink, 6; red, 7-8.

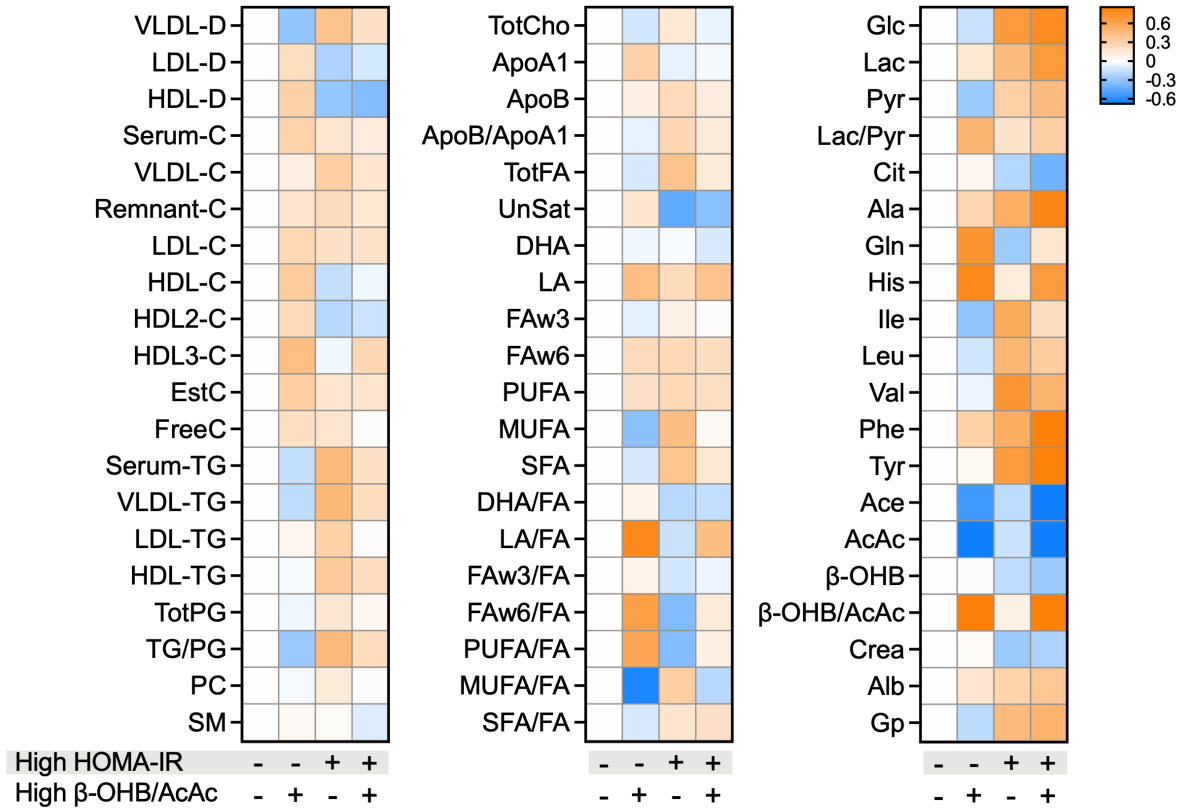

Fig. S5. Insulin resistance and hepatic mitochondrial redox state additively increase serum glycolytic intermediates and aromatic amino acids. A heatmap showing Z-scores of serum metabolomics variables in the groups based on sex-specific medians of HOMA-IR and β-OHB/AcAc. Blue color denotes a negative and orange color a positive difference relative to the 'Low HOMA-IR, Low β-OHB/AcAc' group. VLDL, very low-density lipoprotein; D, diameter; LDL, low-density lipoprotein; HDL, high-density lipoprotein; C, cholesterol; EstC, cholesterol ester; TG, triglyceride; PG, phosphoglyceride; Apo, apolipoprotein; TotFA, total fatty acids; UnSat, unsaturation; LA, linoleic acid; FAw6, omega-6 fatty acid; PUFA, polyunsaturated fatty acid; MUFA, monounsaturated fatty acid; SFA, saturated fatty acid; Lac, lactate; Pyr, pyruvate; Cit, citrate; Ala, alanine; Ile, isoleucine; Leu, leucine; Val, valine; Phe, phenylalanine; Tyr, tyrosine; AcAc; acetoacetate; β-OHB, β-hydroxybutyrate; Gp, glycoprotein acetyls.

SUPPLEMENTARY TABLES

Table S1. Clinical characteristics of the cohorts.					
	Discovery cohort	*Validation cohort*	*Non-bariatric cohort*	*Adipose tissue lipolysis cohort*	*Hepatic de novo lipogenesis cohort*
Number, n	284	208	252	41	61
Age, years	49±1	47±1	48±1	49±2	50±1
Sex, % women	72	70	68	63	66
BMI, kg/m^2	43±1	44±1	30±1	30±1	31±1
Steatosis[1], n, 0/1/2/3	98/131/33/22	82/71/33/22	N/A[3]	N/A[4]	N/A[5]
Ballooning[1], n, 0/1/2	250/26/8	152/52/4	N/A[3]	N/A[4]	N/A[5]
Lobular inflammation[1], n, 0/1/2	242/35/7	133/58/17	N/A[3]	N/A[4]	N/A[5]
Fibrosis[1], n, 0/1/2/3/4	169/96/11/5/3	119/75/10/2/2	N/A[3]	N/A[4]	N/A[5]
Intrahepatic triglyceride content[2], %	N/A	N/A	5.4±0.5	4.8±0.9	5.3±0.8
[1]Determined by liver histology. [2]Determined by proton magnetic resonance spectroscopy. [3]FIB-4 index 1.3±0.1, [4]FIB-4 index 1.1±0.1, [5]FIB-4 index 1.2±0.1. Data are in n (%) or in mean±SEM.					

Table S2. NMR variables in the entire cohort and their correlations with HOMA-IR and Genetic Risk Score (GRS).

	Entire cohort		HOMA-IR				GRS			
	Median	IQR	Beta	Lower 95%	Upper 95%	FDR	Beta	Lower 95%	Upper 95%	FDR
VLDL-D (nm)	39.08	2.07	**0.240**	0.127	0.349	2.12E-04	**-0.135**	-0.197	-0.023	
LDL-D (nm)	24.55	0.22	-0.106	-0.210	0.003		**0.139**	0.028	0.195	
HDL-D (nm)	9.43	0.22	**-0.211**	-0.317	-0.101		**0.118**	0.011	0.180	
Serum-C (mmol/L)	4.20	1.15	0.109	-0.003	0.219		-0.004	-0.090	0.083	
VLDL-C (mmol/L)	0.79	0.43	**0.190**	0.071	0.308	4.79E-03	-0.050	-0.134	0.052	
Remnant-C (mmol/L)	1.46	0.66	**0.160**	0.044	0.275	1.18E-02	-0.017	-0.105	0.077	
LDL-C (mmol/L)	1.69	0.58	**0.129**	0.015	0.242	3.81E-02	-0.036	-0.119	0.060	
HDL-C (mmol/L)	1.02	0.36	-0.066	-0.175	0.044		0.075	-0.025	0.147	
HDL2-C (mmol/L)	0.65	0.29	-0.109	-0.217	0.000		**0.109**	0.003	0.174	
HDL3-C (mmol/L)	0.39	0.11	0.055	-0.063	0.173		-0.044	-0.129	0.057	
EstC (mmol/L)	2.90	0.84	**0.120**	0.009	0.230	4.62E-02	-0.006	-0.092	0.082	
FreeC (mmol/L)	1.30	0.33	0.087	-0.025	0.199		0.004	-0.084	0.091	
Serum-TG (mmol/L)	1.45	0.80	**0.249**	0.131	0.361	1.72E-04	-0.095	-0.167	0.013	
VLDL-TG (mmol/L)	1.02	0.68	**0.260**	0.143	0.372	1.01E-04	-0.105	-0.175	0.005	
LDL-TG (mmol/L)	0.18	0.04	**0.137**	0.017	0.256		-0.044	-0.129	0.058	
HDL-TG (mmol/L)	0.14	0.06	**0.177**	0.056	0.296	8.03E-03	-0.007	-0.100	0.088	
TotPG (mmol/L)	1.93	0.43	0.110	-0.010	0.230		-0.024	-0.113	0.075	
TG/PG	0.69	0.34	**0.235**	0.124	0.343	1.93E-04	**-0.110**	-0.175	-0.004	
PC (mmol/L)	1.97	0.42	0.085	-0.035	0.204		-0.003	-0.096	0.091	
SM (mmol/L)	0.46	0.09	0.021	-0.091	0.133		-0.005	-0.091	0.084	
TotCho (mmol/L)	2.48	0.43	0.089	-0.031	0.208		-0.014	-0.105	0.082	
ApoA1 (g/L)	1.24	0.18	-0.002	-0.110	0.107		0.066	-0.032	0.138	
ApoB (g/L)	0.73	0.19	**0.166**	0.048	0.282	1.07E-02	-0.055	-0.136	0.048	
ApoB/ApoA1	0.59	0.16	**0.171**	0.052	0.288	8.94E-03	-0.097	-0.171	0.013	
TotFA (mmol/L)	11.56	2.92	**0.220**	0.100	0.338	1.08E-03	-0.073	-0.153	0.035	
UnSat	1.18	0.09	**-0.239**	-0.355	-0.120	3.70E-04	0.075	-0.032	0.153	
DHA (mmol/L)	0.11	0.07	0.036	-0.085	0.157		-0.038	-0.126	0.064	
LA (mmol/L)	2.51	0.67	**0.170**	0.054	0.281	8.31E-03	-0.033	-0.116	0.062	
FAw3 (mmol/L)	0.41	0.17	0.119	-0.002	0.234		-0.056	-0.137	0.047	
FAw6 (mmol/L)	3.41	0.78	**0.172**	0.055	0.281	8.18E-03	-0.048	-0.127	0.051	
PUFA (mmol/L)	3.82	0.90	**0.180**	0.062	0.290	6.22E-03	-0.058	-0.136	0.043	
MUFA (mmol/L)	3.62	1.22	**0.215**	0.095	0.333	1.33E-03	-0.069	-0.150	0.037	
SFA (mmol/L)	4.15	1.20	**0.227**	0.106	0.345	7.69E-04	-0.088	-0.165	0.022	
DHA/FA (%)	0.01	0.00	-0.076	-0.198	0.046		0.007	-0.090	0.101	
LA/FA (%)	0.21	0.05	-0.045	-0.157	0.068		0.073	-0.030	0.147	
FAw3/FA (%)	0.03	0.01	-0.032	-0.153	0.089		0.006	-0.090	0.100	
FAw6/FA (%)	0.29	0.04	**-0.166**	-0.274	-0.054	8.33E-03	0.091	-0.013	0.160	
PUFA/FA (%)	0.33	0.05	**-0.155**	-0.265	-0.040	1.28E-02	0.087	-0.018	0.159	
MUFA/FA (%)	0.31	0.04	0.105	-0.007	0.217		-0.043	-0.123	0.052	
SFA/FA (%)	0.36	0.02	**0.158**	0.035	0.277	1.82E-02	**-0.124**	-0.196	-0.005	
Glc (mmol/L)	4.18	0.88	**0.449**	0.353	0.541		**-0.095**	-0.151	-0.004	
Lac (mmol/L)	0.92	0.37	**0.221**	0.103	0.332	7.81E-04	-0.007	-0.096	0.084	
Pyr (mmol/L)	0.11	0.04	**0.186**	0.069	0.303	5.02E-03	**-0.117**	-0.187	-0.003	
Lac/Pyr	8.72	3.01	0.064	-0.060	0.186		**0.124**	0.004	0.197	
Cit (mmol/L)	0.15	0.03	**-0.140**	-0.261	-0.017	3.76E-02	0.014	-0.084	0.108	
Ala (mmol/L)	0.35	0.06	**0.232**	0.119	0.346	3.18E-04	-0.028	-0.112	0.066	
Gln (mmol/L)	0.41	0.08	-0.117	-0.236	0.004		0.084	-0.026	0.162	
His (mmol/L)	0.05	0.01	0.100	-0.023	0.224		0.019	-0.081	0.113	
Ile (mmol/L)	0.05	0.02	**0.283**	0.175	0.388	8.99E-06	**-0.115**	-0.177	-0.009	
Leu (mmol/L)	0.07	0.02	**0.258**	0.146	0.364	6.77E-05	-0.090	-0.158	0.013	
Val (mmol/L)	0.16	0.04	**0.263**	0.150	0.376	5.86E-05	-0.071	-0.147	0.030	
Phe (mmol/L)	0.06	0.01	**0.273**	0.157	0.385	7.01E-05	0.066	-0.036	0.143	
Tyr (mmol/L)	0.05	0.01	**0.389**	0.279	0.496	7.85E-10	0.018	-0.071	0.100	
Ace (mmol/L)	0.05	0.01	0.013	-0.105	0.130		-0.067	-0.145	0.038	
AcAc (mmol/L)	0.07	0.07	**-0.170**	-0.291	-0.047	1.18E-02	-0.094	-0.173	0.019	
β-OHB (mmol/L)	0.19	0.16	**-0.132**	-0.255	-0.008	4.82E-02	-0.017	-0.110	0.083	
β-OHB/AcAc	2.80	1.51	0.095	-0.026	0.216		**0.148**	0.026	0.216	1.26E-02
Crea (mmol/L)	0.06	0.01	**-0.175**	-0.287	-0.061		-0.006	-0.093	0.084	
Alb (signal area)	0.08	0.01	**0.236**	0.115	0.357		-0.051	-0.136	0.053	
Gp (mmol/L)	1.22	2.80	**0.220**	0.104	0.332	7.48E-04	**-0.132**	-0.196	-0.017	

Betas are calculated by linear regression, adjusted for age, sex, body mass index, diabetes and lipid-lowering medication. Additionally, HOMA-IR analyses are adjusted for GRS and *vice versa*. False discovery rate (FDR) adjusted values are calculated only for variables which were included in the principal components that were significantly correlated with HOMA-IR or GRS. Beta values in bold denote nominal significances; red color a positive and blue a negative correlation. VLDL, very low-density lipoprotein; D, diameter; LDL, low-density lipoprotein; HDL, high-density lipoprotein; C, cholesterol; EstC, cholesterol ester; FreeC, free cholesterol; TG, triglyceride; TotPG, total phosphoglycerides; PC, phosphatidylcholine; SM, sphingomyelin; TotCho, total cholesterol; Apo, apolipoprotein; TotFA, total fatty acids; UnSat, unsaturation; DHA, docosahexaenoic acid; LA, linoleic acid; FAw3, omega-3 fatty acid; FAw6, omega-6 fatty acid; PUFA, polyunsaturated fatty acid; MUFA, monounsaturated fatty acid; SFA, saturated fatty acid; Glc, glucose; Lac, lactate; Pyr, pyruvate; Cit, citrate; Ala, alanine; Gln, glutamine; His, histidine; Ile, isoleucine; Leu, leucine; Val, valine; Phe, phenylalanine; Tyr, tyrosine; Ace, acetate; AcAc; acetoacetate; β-OHB, β-hydroxybutyrate; Crea, creatinine; Alb, albumin; Gp, glycoprotein acetyls.

Table S3. Principal Component Matrix.

	Component											
	1	2	3	4	5	6	7	8	9	10	11	12
TotFA	0.980											
SFA	0.977											
MUFA	0.937											
VLDL-C	0.922											
ApoB	0.901											
Serum-TG	0.882											
VLDL-TG	0.870											
Remnant-C	0.853											
PUFA	0.816	0.502										
FAw6	0.812	0.488										
TotPG	0.794											
ApoB/ApoA1	0.788											
PC	0.776	0.413										
LDL-TG	0.765											
TotCho	0.763											
HDL-TG	0.740											
FreeC	0.721	0.600										
TG/PG	0.721	-0.612										
LA	0.703	0.463										
VLDL-D	0.696	-0.553										
Serum-C	0.693	0.665										
UnSat	-0.686	0.447	0.403									
Gp	0.655											
LDL-C	0.637	0.543										
FAw3	0.588	0.406	0.587									
Ile	0.540	-0.530										
SFA/FA	0.457									-0.422		
Leu	0.433	-0.407										
ApoA1		0.844										
HDL-C		0.792										
HDL2-C		0.758		-0.411								
MUFA/FA	0.461	-0.725										
LDL-D		0.708										
PUFA/FA	-0.559	0.689										
HDL-D		0.688										
SM	0.497	0.682										
EstC	0.677	0.680										
FAw6/FA	-0.588	0.622										
LA/FA		0.546		0.517								
HDL3-C		0.449										
Glc												
DHA/FA		0.452	0.717									
FAw3/FA		0.472	0.717			-0.417						
DHA		0.428	0.666									
AcAc					-0.692	0.406						
His					0.607							
Ala					0.563							
β-OHB/AcAc					0.552				0.402		-0.415	
β-OHB					-0.469	0.459						
Tyr					0.422							
Phe					0.407							
Val						0.441						
Cit						0.435						
Lac							0.622					
Gln								0.465				
Ace												
Alb												
Pyr	0.437									0.442		
Lac/Pyr												
Crea								0.407				0.578

Values denote correlations between the NMR variables and principal components. Only correlations above 0.4 are shown. VLDL, very low-density lipoprotein; D, diameter; LDL, low-density lipoprotein; HDL, high-density lipoprotein; C, cholesterol; EstC, cholesterol ester; FreeC, free cholesterol; TG, triglyceride; TotPG, total phosphoglycerides; PC, phosphatidylcholine; SM, sphingomyelin; TotCho, total cholesterol; Apo, apolipoprotein; TotFA, total fatty acids; UnSat, unsaturation; DHA, docosahexaenoic acid; LA, linoleic acid; FAw3, omega-3 fatty acid; FAw6, omega-6 fatty acid; PUFA, polyunsaturated fatty acid; MUFA, monounsaturated fatty acid; SFA, saturated fatty acid; Glc, glucose; Lac, lactate; Pyr, pyruvate; Cit, citrate; Ala, alanine; Gln, glutamine; His, histidine; Ile, isoleucine; Leu, leucine; Val, valine; Phe, phenylalanine; Tyr, tyrosine; Ace, acetate; AcAc; acetoacetate; β-OHB, β-hydroxybutyrate; Crea, creatinine; Alb, albumin; Gp, glycoprotein acetyls.

Table S4. Sensitivity analysis.				
	Beta	Lower 95 %	Upper 95 %	*P*-value
SAF score				
Full GRS	0.200	0.055	0.209	0.001
GRS without *PNPLA3*	0.157	0.023	0.157	0.009
GRS without *TM6SF2*	0.183	0.041	0.187	0.002
GRS without *MBOAT7*	0.189	0.041	0.177	0.002
GRS without *HSD17B13*	0.200	0.052	0.195	0.001
GRS without *MARC1*	0.162	0.025	0.160	0.008
β-OHB/AcAc				
Full GRS	0.159	0.052	0.342	0.008
GRS without *PNPLA3*	0.149	0.036	0.287	0.012
GRS without *TM6SF2*	0.120	0.003	0.278	0.045
GRS without *MBOAT7*	0.159	0.045	0.299	0.008
GRS without *HSD17B13*	0.118	0.001	0.271	0.048
GRS without *MARC1*	0.166	0.052	0.304	0.006
Sensitivity analyses of the association of the full GRS or alternative GRSs excluding one genetic risk variant at a time with the SAF score and β-OHB/AcAc. Standardized beta regression coefficients and 95% confidence intervals are reported. Analyses were adjusted for age, sex and BMI.				

Table S5. Clinical characteristics of the participants in groups based on sex-specific medians of HOMA-IR and β-OHB/AcAc.

	Low HOMA-IR, Low β-OHB/AcAc	Low HOMA-IR, High β-OHB/AcAc	High HOMA-IR, Low β-OHB/AcAc	High HOMA-IR, High β-OHB/AcAc
Group size, n	72	70	70	72
Age, years	50 (10)	48 (11)	49 (15)	50 (14)
Women, n (%)	49 (68)	55 (79)	55 (79)	48 (67)
Body mass index, kg/m^2	41.4 (9.4)	40.6 (7.8)	44.4 (8.3)	44.4 (8.2)***
Waist circumference, cm	121.8 (17.3)	117.3 (24.0)	128.0 (23.0)	131 (17.3)***
fP-Glucose, mmol/L	5.5 (1.3)	5.4 (0.9)	6.0 (1.1)	6.2 (1.4)***
fS-Insulin, mU/L	7.5 (4.9)	8.3 (4.0)	19.0 (8.9)	18.0 (10.0)***
Hemoglobin A_{1C}, %	5.7 (0.7)	5.5 (0.7)	5.8 (0.8)	5.9 (0.7)***
fP-Total cholesterol, mmol/L	4.2 (1.2)	4.3 (1.3)	4.0 (1.1)	4.2 (1.2)
fP-HDL cholesterol, mmol/L	1.15 (0.48)	1.21 (0.39)	1.10 (0.37)	1.18 (0.44)
fP-LDL cholesterol, mmol/L	2.4 (1.1)	2.6 (1.1)	2.4 (1.4)	2.5 (1.1)
fP-Triglycerides, mmol/L	1.12 (0.82)	1.07 (0.52)	1.37 (0.61)	1.27 (0.63)***
P-Alanine aminotransferase, U/L	31 (20)	28 (25)	34 (27)	37 (21)
P-Aspartate aminotransferase, U/L	30 (14)	29 (13)	28 (15)	30 (12)
P-Gamma-glutamyltransferase, U/L	25 (26)	28 (26)	28 (33)	36 (33)*
P-Albumin, g/L	38.3 (3.2)	37.9 (2.8)	38.6 (4.2)	38.2 (3.9)
B-Platelets, 10^9/L	235 (68)	253 (74)	251 (92)	268 (75)*
Type 2 diabetes, n (%)	27 (38)	21 (30)	34 (49)	37 (51)*
NAFLD, n (%)	39 (54)	37 (53)	53 (76)	58 (81)***
NASH, n (%)	2 (3)	5 (7)	8 (11)	15 (21)**
PNPLA3 rs738409 (CC/CG/GG), n	42/27/3	40/23/7	40/27/3	40/29/3
TM6SF2 rs58542926 (CC/CT/TT), n	66/5/1	56/14/0	67/2/1	59/13/0*
MBOAT7 rs641738 (CC/CT/TT), n	26/37/9	23/30/17	27/33/10	19/39/14
HSD17B13 rs72613567 (AA/A0/00), n	2/34/36	1/21/48	3/22/45	3/25/44
MARC1 rs2642438 (AA/AG/GG), n	5/33/34	4/19/47	2/28/40	7/25/40

Categorical data are in n (%) and continuous data in median (interquartile range). Significances were determined by Kruskal-Wallis analysis of variance test for continuous or Pearson's χ2 test for categorical variables. *P≤0.05, **P≤0.01, ***P≤0.001. β-OHB, β-hydroxybutyrate; AcAc, acetoacetate; HOMA-IR, homeostasis assessment of insulin resistance; f, fasting; P, plasma; S, serum; B, blood.

Supplementary materials and methods

Human participants

We recruited a total of 284 participants (207 women, mean age 49±1 years, BMI 43±1 kg/m^2, 187 with NAFLD and 30 with NASH; *Discovery cohort*, Table S1) amongst those undergoing laparoscopic bariatric surgery at the Helsinki University Hospital (Helsinki, Finland). The following inclusion criteria were employed:

1. Age range from 18 to 75 years;
2. Alcohol consumption <20 g/day for women and <30 g/day for men;
3. No known acute or chronic disease other than obesity, type 2 diabetes, NAFLD or hypertension on the basis of medical history, physical examination and blood count, plasma creatinine and electrolyte concentrations;
4. No clinical or biochemical evidence of liver disease other than NAFLD, or clinical signs or symptoms of inborn errors of metabolism;
5. No history or current use of hepatotoxic compounds;
6. No pregnancy or breastfeeding in women.

The week preceding the surgery, the subjects arrived at the Clinical Research Unit after an overnight fast. A history and physical examination were performed to review the inclusion criteria. Body weight, height, BMI and waist circumference were assessed as described [1]. Blood samples were obtained from an antecubital vein for genotyping, NMR metabolomics and routine biochemistry (see below). An additional 208 participants (mean±sem age 47±1 years, BMI 44±1 kg/m^2, 145 women; *Validation cohort*, Table S1) were recruited amongst those undergoing laparoscopic bariatric surgery at the Kuopio University Hospital (Kuopio, Finland)

using the same inclusion and exclusion criteria [2]. Another 252 participants that were not undergoing bariatric surgery were also recruited using the same inclusion and exclusion criteria (mean±sem age 48±1 years, BMI 30±1 kg/m^2, 172 women, FIB-4 1.3±0.1; *Non-bariatric cohort*, Table S1). The study protocols were approved by the ethics committees of the Hospital District of Helsinki and Uusimaa (Helsinki, Finland) the Hospital District of Northern Savo (Kuopio, Finland). The study was conducted in accordance with the Declaration of Helsinki. Each participant provided written informed consent after being explained the nature and potential risks of the study.

Hepatic *de novo* lipogenesis

A total of 61 participants who were not undergoing liver biopsy were recruited for quantification of hepatic *de novo* lipogenesis (DNL) using the same inclusion criteria (Table S1) [3, 4]. The day before the metabolic study, a blood sample was taken for the measurement of background enrichment of ^2H in plasma water as well as VLDL-TG palmitate for the measurement of DNL. Subjects then underwent IHTG measurement by proton magnetic resonance spectroscopy (^1H-MRS, see below). The following morning, subjects arrived at the clinical research unit after an overnight fast and after consuming deuterated water (^2H_2O) (3 g/kg body water) the evening prior to the study day, in order to achieve a plasma water enrichment of 0.3% for the measurement of DNL. Fasting hepatic DNL was measured from incorporation of deuterium of ^2H_2O in plasma water (Finnigan GasBench-II, ThermoFisher Scientific, UK) into palmitate in VLDL-TG using gas chromatography/mass spectrometry (GC/MS) with monitoring ions with mass-to-charge ratios (m/z) of 270 (M+0) and 271 (M+1) [5]. For the calculation of DNL in VLDL-TG using the mass isotopomer distributions, the maximum number of deuterium molecules synthesized from plasma palmitate was assumed

to be 22 [6]. When constant enrichment in the precursor pool (plasma water) was obtained, F was the enrichment of palmitate synthesized during the time between the loading dose of $^{2}H_2O$ and the collection time. When isotopic equilibrium in the product pool (palmitate) was obtained, F was constant. F = plasma palmitate enrichment/(22 × plasma deuterium enrichment). The percentage of DNL (%DNL) was calculated by multiplying F by 100%. VLDL was isolated by ultracentrifugation as described [4].

Adipose tissue lipolysis

Insulin action on plasma NEFA and glycerol rate of appearance (R_a) were determined using the euglycemic hyperinsulinemic clamp technique as previously described [4, 7] in 41 participants recruited using the same inclusion criteria as above (Table S1). The duration of the insulin infusion was 120 min (120-240 min) and rate of the continuous insulin infusion was 0.4 mU/kg·min. Before start of the infusions, two 18 gauge catheters (Venflon, Viggo-Spectramed, Helsingborg, Sweden) were inserted, one in a left antecubital vein and another retrogradely in a heated (+65 °C) dorsal hand vein for sampling of arterialized venous blood for insulin (0, 120, 180 and 240 min) and concentrations of NEFA and glycerol and its isotopic enrichment (0, 100, 120, 130, 140, 150, 180, 240 min). The rate of whole-body lipolysis and effect of insulin on lipolysis were determined by infusing [$^{2}H_5$]glycerol for 120 min before (0-120 min) and for 120 min during the insulin infusion (120-240 min).

Intrahepatic triglycerides

IHTG content was measured by proton magnetic resonance spectroscopy (^{1}H-MRS) on a 1.5T clinical MR imager (Siemens Avanto^{fit}, Erlangen, Germany). Spectra were analyzed with jMRUI v5.2 software (www.jmrui.eu) utilizing AMARES algorithm as described [4].

Genotyping and the genetic risk score

Genotyping of *PNPLA3* rs738409, *TM6SF2* rs58542926, *MBOAT7* rs641738, *HSD17B13* rs72613567, *MARC1* rs2642438 and *GCKR* rs1260326 was performed using the TacMan PCR methodology according to the manufacturer's instructions (Applied Biosystems, Foster City, CA, USA). The genetic risk score (GRS) was calculated as the unweighted sum of effect alleles in NAFLD-predisposing polymorphisms (*PNPLA3* rs738409-G, *TM6SF2* rs58542926-T and *MBOAT7* rs641738-T) and reference alleles in protective polymorphisms (*HSD17B13* rs72613567-0 and *MARC1* rs2642438-G) as previously described [8-10].

Nuclear magnetic resonance metabolomics

A high-throughput NMR metabolomics platform (AVANCE III 500 MHz and AVANCE III 600 MHz, Bruker, Karlsruhe, Germany) was used for the quantification of serum lipid and metabolite measures that represent a broad molecular signature of systemic metabolism. The experimental setup allows for the simultaneous quantification of routine lipids, lipoprotein subclass distributions, fatty acids, as well as low–molecular weight metabolites, such as amino acids and glycolysis-related metabolites and ketone bodies in absolute concentration units [11]. The methodological characteristics of the platform have been described elsewhere [11-13]. Over the last 10 years, this particular platform has become common in epidemiology and genetics [14].

Hepatic mitochondrial redox state

In liver mitochondria, the β-hydroxybutyrate dehydrogenase enzyme reduces acetoacetate to β-hydroxybutyrate [15]. The ratio of concentrations of β-hydroxybutyrate to acetoacetate is in

equilibrium with the ratio of free reduced nicotinamide adenine dinucleotide dehydrogenase (NADH) to oxidized nicotinamide adenine dinucleotide (NAD^+) in the mitochondria [16] as shown by the equation: β-hydroxybutyrate + $NAD^+ \leftrightarrow$ acetoacetate + NADH + H^+. Thus, the ratio of β-hydroxybutyrate to acetoacetate reflects the free NADH/NAD^+ ratio in the mitochondria [16]. Since β-hydroxybutyrate and acetoacetate are synthesized exclusively in the liver and pass freely through the cell membrane, their ratio provides a liver-specific marker of the intramitochondrial redox state (NADH/NAD^+) [16-19].

In the cytosol of hepatic and extrahepatic cells, lactate dehydrogenase reduces pyruvate to lactate [16]. The ratio of the concentrations of lactate to pyruvate is in equilibrium with the ratio of free NADH to NAD^+ in cytosol [16] as shown by the formula: lactate + $NAD^+ \leftrightarrow$ pyruvate + NADH + H^+. Thus, the ratio of lactate to pyruvate reflects the free NADH/NAD^+ ratio in the cytosol [16]. However, unlike the ketone bodies, lactate and pyruvate are not produced exclusively by the liver, and thus the ratio of lactate and pyruvate reflects the cytosolic NADH/NAD^+ ratio of many tissues.

Analytical methods

Fasting plasma glucose was measured using the hexokinase method on an autoanalyzer (Roche Diagnostics Hitachi 917, Hitachi Ltd., Tokyo, Japan). Serum insulin concentration was determined by time-resolved fluoroimmunoassay using Insulin Kit (AUTOdelfia, Wallac, Turku, Finland). IR was determined by using the homeostatic model assessment of IR (HOMA-IR), calculated using the formula: serum insulin (mU/L) x plasma glucose (mmol/L) / 22.5 [20]. Hemoglobin A1c was measured with an immunoturbidometric method (Abbott Laboratories, Chicago, IL, USA) and plasma triglyceride, total cholesterol, LDL and HDL cholesterol

concentrations using enzymatic kits and an autoanalyzer (Roche Diagnostics Hitachi 917, Hitachi Ltd., Tokyo, Japan). Plasma alanine aminotransferase, aspartate aminotransferase and gamma-glutamyltransferase activities were determined using photometric International Federation of Clinical Chemistry methods (Abbott Laboratories). Plasma albumin was measured using a photometric method on an autoanalyzer (Modular Analytics EVO; Hitachi High-Technologies Corporation, Tokyo, Japan). Blood counts and platelets were assessed by impedance, flow cytometric, and photometric assays (XN10, Sysmex).

Liver biopsies and histology

In the *Discovery cohort*, on the day of surgery, a clinically indicated wedge biopsy of the liver was obtained and assessed by an experienced liver pathologist for steatosis, inflammation and fibrosis according to the SAF score [21]. Steatosis was scored by the amount of large or medium-sized lipid droplets from 0 to 3 (0: <5%, 1: 5-33%, 2: 34-66%, 3: >67%). Ballooning was graded from 0 to 2 (0: normal hepatocytes, 1: clusters of hepatocytes with rounded shape and pale cytoplasm, 2: same as 1 with at least two-fold enlarged hepatocytes). Lobular inflammation was graded from 0 to 2 as the number of foci with two or more inflammatory cells within the lobule (0: none, 1: <3 foci, 2: >3 foci per 20x). Activity grade (0-4) was calculated as the unweighted sum of ballooning (0-2) and lobular inflammation (0-2). Fibrosis was staged from 0 to 4 (0: none, 1: perisinusoidal or periportal fibrosis, 2: perisinusoidal and periportal fibrosis without bridging, 3: bridging fibrosis, 4: cirrhosis). The total SAF score (0-11) was calculated as the unweighted sum of steatosis (0-3), activity (0-4) and fibrosis (0-4). In the Validation cohort, lobular inflammation was graded from 0 to 3 (0: no foci, 1: <2 foci, 2: 2-4 foci, 3: >4 foci per 20x field) and portal inflammation was graded from 0 to 1 (0: none to minimal, 1: greater than minimal). NAFLD was defined as the number of hepatocytes with

macrovesicular steatosis exceeding 5%. NASH was defined as steatosis >0, ballooning >0 and lobular inflammation >0.

To investigate the effect of IR on liver histology and metabolism, the participants were divided into six quantiles based on sex-specific HOMA-IR (*H1-H6*). To investigate the effect of polygenic risk on liver histology and metabolism, the same individuals were also divided into six groups based on the GRS (*G1-G6*, Fig. 2A). To investigate the effect of hepatic mitochondrial redox state and IR on liver histology and metabolism in individuals with NAFLD, the subjects with NAFLD were divided into four non-overlapping groups based on sex-specific medians of HOMA-IR and β-OHB/AcAc ('Low HOMA-IR, Low β-OHB/AcAc', 'Low HOMA-IR, High β-OHB/AcAc', 'High HOMA-IR, Low β-OHB/AcAc' and 'High HOMA-IR, High β-OHB/AcAc', Table S5).

Statistical methods

The Kruskal-Wallis analysis of variance test was used to compare continuous characteristics and Pearson's χ2 test to compare categorical characteristics between the groups. Due to an a priori hypothesis for increasing values as a function of increasing group number (*H1-H6* and *G1-G6*), the Jonckheere-Terpstra and Pearson's χ2 trend tests were used for HOMA-IR, GRS and liver histology.

None of the NMR variables had missing values. Data was normal transformed by using the rank-based inverse normal transformation, *i.e.* first mapped to the probability scale by replacing the observed values with fractional ranks followed by transformation into Z-scores (mean 0, standard deviation 1) using the probit function.

After sampling adequacy was confirmed using the Kaiser-Meyer-Olkin Measure of Sampling Adequacy test (>0.8) and Bartlett's test of Sphericity (P<0.001), principal component analysis of the NMR metabolomics data was performed to reduce dimensionality of the data. Principal components with Eigenvalue > 1 were included in further analyses, and NMR variables with correlation >0.4 with individual principal components were considered to be part of that component. Factor scores of each principal component were calculated by using the regression method.

To determine which principal components associated with HOMA-IR and GRS, linear regression analyses were performed between principal component factor scores and HOMA-IR and GRS, adjusted for age, sex, BMI, diabetes and lipid-lowering medication. For HOMA-IR, analyses were also adjusted for GRS and vice versa. Next, to determine which individual NMR metabolites within the principal components associated with HOMA-IR and GRS, linear regression analyses were performed between NMR metabolites in significantly associated principal components and HOMA-IR and GRS, adjusted for age, sex, BMI, diabetes and lipid-lowering medication. For HOMA-IR, analyses were also adjusted for GRS and *vice versa*.

Associations between the variables that associated with HOMA-IR and liver histology were determined by linear regression, adjusted for age, sex, BMI, diabetes, lipid-lowering medication and GRS. Associations between variables that associated with the GRS and liver histology were determined by linear regression, adjusted for age, sex, BMI, diabetes, lipid-lowering medication and HOMA-IR. Associations between β-OHB/AcAc and HOMA-IR and liver histology were determined by linear regression, adjusted for age, sex, BMI and diabetes.

Multiple testing was corrected by using the Benjamini-Hochberg false discovery rate (FDR) method, with FDR 0.05 as a threshold for significance. Data are reported in medians (interquartile range, IQR), means ± SEM or in numbers (n).

With respect to sample size and adequate power, we have previously observed highly significant differences in serum NMR metabolomics data in genotype-based groups of only 18 individuals [22].

Statistical analyses were performed using GraphPad Prism 8.1.2 for Mac OS X (GraphPad Software, La Jolla, CA, USA), R version 3.6.0 (R Foundation for Statistical Computing, Vienna, Austria), Microsoft Excel for Mac 16.35 (Microsoft, Redmond, WA, USA) and IBM SPSS for Mac version 25 (IBM, Armonk, NY, USA). A P-value of equal or less than 0.05 was considered to be statistically significant.

Supplementary references

[1] Luukkonen PK, Dufour S, Lyu K, Zhang XM, Hakkarainen A, Lehtimaki TE, et al. Effect of a ketogenic diet on hepatic steatosis and hepatic mitochondrial metabolism in nonalcoholic fatty liver disease. Proc Natl Acad Sci U S A 2020;117:7347-7354.

[2] Mannisto VT, Simonen M, Hyysalo J, Soininen P, Kangas AJ, Kaminska D, et al. Ketone body production is differentially altered in steatosis and non-alcoholic steatohepatitis in obese humans. Liver Int 2015;35:1853-1861.

[3] Luukkonen PK, Tukiainen T, Juuti A, Sammalkorpi H, Haridas PAN, Niemela O, et al. Hydroxysteroid 17-beta dehydrogenase 13 variant increases phospholipids and protects against fibrosis in nonalcoholic fatty liver disease. JCI Insight 2020;5.

[4] Luukkonen PK, Sadevirta S, Zhou Y, Kayser B, Ali A, Ahonen L, et al. Saturated Fat Is More Metabolically Harmful for the Human Liver Than Unsaturated Fat or Simple Sugars. Diabetes Care 2018;41:1732-1739.

[5] Semple RK, Sleigh A, Murgatroyd PR, Adams CA, Bluck L, Jackson S, et al. Postreceptor insulin resistance contributes to human dyslipidemia and hepatic steatosis. J Clin Invest 2009;119:315-322.

[6] Diraison F, Pachiaudi C, Beylot M. Measuring lipogenesis and cholesterol synthesis in humans with deuterated water: use of simple gas chromatographic/mass spectrometric techniques. J Mass Spectrom 1997;32:81-86.

[7] Sevastianova K, Kotronen A, Gastaldelli A, Perttila J, Hakkarainen A, Lundbom J, et al. Genetic variation in PNPLA3 (adiponutrin) confers sensitivity to weight loss-induced decrease in liver fat in humans. Am J Clin Nutr 2011;94:104-111.

[8] Gellert-Kristensen H, Nordestgaard BG, Tybjaerg-Hansen A, Stender S. High Risk of Fatty Liver Disease Amplifies the Alanine Transaminase-Lowering Effect of a HSD17B13 Variant. Hepatology 2020;71:56-66.

[9] Gellert-Kristensen H, Richardson TG, Davey Smith G, Nordestgaard BG, Tybjaerg-Hansen A, Stender S. Combined Effect of PNPLA3, TM6SF2, and HSD17B13 Variants on Risk of Cirrhosis and Hepatocellular Carcinoma in the General Population. Hepatology 2020.

[10] Mancina RM, Dongiovanni P, Petta S, Pingitore P, Meroni M, Rametta R, et al. The MBOAT7-TMC4 Variant rs641738 Increases Risk of Nonalcoholic Fatty Liver Disease in Individuals of European Descent. Gastroenterology 2016;150:1219-1230 e1216.

[11] Soininen P, Kangas AJ, Wurtz P, Suna T, Ala-Korpela M. Quantitative serum nuclear magnetic resonance metabolomics in cardiovascular epidemiology and genetics. Circ Cardiovasc Genet 2015;8:192-206.

[12] Inouye M, Kettunen J, Soininen P, Silander K, Ripatti S, Kumpula LS, et al. Metabonomic, transcriptomic, and genomic variation of a population cohort. Mol Syst Biol 2010;6:441.

[13] Soininen P, Kangas AJ, Wurtz P, Tukiainen T, Tynkkynen T, Laatikainen R, et al. High-throughput serum NMR metabonomics for cost-effective holistic studies on systemic metabolism. Analyst 2009;134:1781-1785.

[14] Wurtz P, Kangas AJ, Soininen P, Lawlor DA, Davey Smith G, Ala-Korpela M. Quantitative Serum Nuclear Magnetic Resonance Metabolomics in Large-Scale Epidemiology: A Primer on -Omic Technologies. Am J Epidemiol 2017;186:1084-1096.

[15] Chapman MJ, Miller LR, Ontko JA. Localization of the enzymes of ketogenesis in rat liver mitochondria. J Cell Biol 1973;58:284-306.

[16] Williamson DH, Lund P, Krebs HA. The redox state of free nicotinamide-adenine dinucleotide in the cytoplasm and mitochondria of rat liver. Biochem J 1967;103:514-527.
[17] Burgess SC, Hausler N, Merritt M, Jeffrey FM, Storey C, Milde A, et al. Impaired tricarboxylic acid cycle activity in mouse livers lacking cytosolic phosphoenolpyruvate carboxykinase. J Biol Chem 2004;279:48941-48949.
[18] Madiraju AK, Erion DM, Rahimi Y, Zhang XM, Braddock DT, Albright RA, et al. Metformin suppresses gluconeogenesis by inhibiting mitochondrial glycerophosphate dehydrogenase. Nature 2014;510:542-546.
[19] Madiraju AK, Qiu Y, Perry RJ, Rahimi Y, Zhang XM, Zhang D, et al. Metformin inhibits gluconeogenesis via a redox-dependent mechanism in vivo. Nat Med 2018;24:1384-1394.
[20] Matthews DR, Hosker JP, Rudenski AS, Naylor BA, Treacher DF, Turner RC. Homeostasis model assessment: insulin resistance and beta-cell function from fasting plasma glucose and insulin concentrations in man. Diabetologia 1985;28:412-419.
[21] Bedossa P, Poitou C, Veyrie N, Bouillot JL, Basdevant A, Paradis V, et al. Histopathological algorithm and scoring system for evaluation of liver lesions in morbidly obese patients. Hepatology 2012;56:1751-1759.
[22] Luukkonen PK, Qadri S, Lehtimaki TE, Juuti A, Sammalkorpi H, Penttila AK, et al. The PNPLA3-I148M Variant Confers an Antiatherogenic Lipid Profile in Insulin-resistant Patients. J Clin Endocrinol Metab 2021;106:e300-e315.